Initial Results of ^{68}Ga-FAPI-46 PET/MRI to Assess Response to Neoadjuvant Chemotherapy in Breast Cancer

Philipp Backhaus*[1–3], Matthias C. Burg*[4], Inga Asmus[1], Michaela Pixberg[1], Florian Büther[1,2], Hans-Jörg Breyholz[1], Randy Yeh[3], Stefanie B. Weigel[4], Patricia Stichling[4], Walter Heindel[4], Stefanie Bobe[2,5], Peter Barth[5], Joke Tio[6], and Michael Schäfers[1,2]

[1]*Department of Nuclear Medicine, University Hospital Münster, Münster, Germany;* [2]*European Institute for Molecular Imaging, University of Münster, Münster, Germany;* [3]*Molecular Imaging and Therapy Service, Department of Radiology, Memorial Sloan Kettering Cancer Center, New York City, New York;* [4]*Clinic for Radiology, University Hospital Münster, Münster, Germany;* [5]*Gerhard-Domagk Institute for Pathology, University of Münster, Münster, Germany; and* [6]*Department of Gynecology and Obstetrics, University Hospital Münster, Münster, Germany*

Improving imaging-based response after neoadjuvant chemotherapy (NAC) in breast cancer assessment could obviate histologic confirmation of pathologic complete response (pCR) and facilitate deescalation of chemotherapy or surgery. Fibroblast activation protein inhibitor (FAPI) PET/MRI is a promising novel molecular imaging agent for the tumor microenvironment with intense uptake in breast cancer. We assessed the diagnostic performance of follow-up breast ^{68}Ga-FAPI-46 (^{68}Ga-FAPI) PET/MRI in classifying the response status of local breast cancer and lymph node metastases after completion of NAC and validated this approach immunohistochemically. **Methods:** In women who completed NAC for invasive breast cancer, follow-up ^{68}Ga-FAPI PET/MRI and corresponding fibroblast activation protein (FAP) immunostainings were retrospectively analyzed. Metrics of ^{68}Ga-FAPI uptake and FAP immunoreactivity in women with or without pCR were compared using the Mann–Whitney *U* test. Diagnostic performance to detect remnant invasive cancer was calculated for tracer uptake metrics using receiver-operating-characteristic curves and for masked readers' visual assessment categories of PET/MRI and MRI alone. **Results:** Thirteen women (mean age ± SD, 47 ± 9 y) were evaluated. Seven of the 13 achieved pCR in the breast and 6 in the axilla. FAP immunoreactivity was significantly associated with response status. The ^{68}Ga-FAPI PET/MRI mean breast tumor-to-background ratio was 0.9 (range, 0.6–1.2) for pCR and 2.1 (range, 1.4–3.1) for no pCR ($P = 0.001$). Integrated PET/MRI could classify breast response correctly in all 13 women based on readers' visual assessment or tumor-to-background ratio. Evaluation of MRI alone resulted in at least 2 false-positives. For lymph nodes, PET/MRI readers had at least 2 false-negative classifications, whereas MRI alone resulted in 2 false-negatives and 1 false-positive. **Conclusion:** To our knowledge, this was the first analysis of ^{68}Ga-FAPI PET/MRI for response assessment after NAC for breast cancer. The diagnostic performance of PET/MRI in a small study sample trended toward a gain over MRI alone, clearly supporting future prospective studies.

Key Words: FAPI; PET/MRI; breast cancer; neoadjuvant chemotherapy; deescalation

J Nucl Med 2023; 64:717–723
DOI: 10.2967/jnumed.122.264871

In breast cancer, application of systemic neoadjuvant chemotherapy (NAC) before curative surgery may achieve resectability, increase the frequency of breast-conserving treatment, and reduce the extent of axillary surgery. Moreover, the remission status at the primary cancer site gives valuable implications on prognosis and subsequent therapy decisions (*1*). In German breast centers, neoadjuvant application of chemotherapy rose from 20% to 58% from 2008 to 2017, and the pathologic complete response (pCR) rate rose from 15% to 34% (*2*). Importantly, pCR implies local cure from invasive cancer by NAC alone. Knowledge of pCR status would thus allow for deescalation of therapy—either abbreviation of chemotherapy (*3*) or even omission of breast and axillary surgery (*4*). However, pCR can currently be reliably determined only by histopathologic confirmation, and all patients therefore undergo complete NAC followed by surgery.

Breast MRI has been shown to provide the most accurate preoperative guidance for resection volumes and is sensitive in detecting remnant cancer (*5*). Combinations with breast MRI can increase diagnostic accuracy, such as combination with ultrasound (*6*), biopsies (*7*), machine learning (*8*), or ^{18}F-FDG PET/MRI (*9*). However, no method has yet proven sufficiently accurate and feasible to allow for deescalation of chemotherapy or surgery.

In a recent study, we introduced ^{68}Ga-labeled fibroblast activation protein inhibitor (FAPI) PET as a novel molecular readout for invasive breast cancer in integrated breast PET/MRI (*10*). This technique takes advantage of expression of the fibroblast activation protein (FAP) by cancer-associated fibroblasts in the tumor microenvironment. Further studies have substantiated superior detection of breast cancer lesions of ^{68}Ga-FAPI PET/CT over ^{18}F-FDG (*11,12*). In this study, we aimed to assess the diagnostic performance of follow-up breast ^{68}Ga-FAPI-46 (^{68}Ga-FAPI) PET/MRI in classifying the response status in local breast cancer and lymph node (LN) metastases after completion of NAC and to validate this approach immunohistochemically.

MATERIALS AND METHODS

Patients

We retrospectively analyzed ^{68}Ga-FAPI PET/MRI scans and corresponding FAP immunostainings of women with breast cancer. Patients were referred by their treating oncologist on an individual, clinical basis to support response assessment after NAC. All patients gave

Received Sep. 2, 2022; revision accepted Nov. 1, 2022.
For correspondence or reprints, contact Philipp Backhaus (philipp.backhaus@ukmuenster.de).
*Contributed equally to this work.
Published online Nov. 17, 2022.

written informed consent for ^{68}Ga-FAPI PET/MRI and retrospective scientific analysis. Analysis was approved by the Ethics Committee of the Medical Association of Westphalia–Lippe and the Medical Faculty of the University of Münster (reference number: 2021-408-f-S). This study included all breast cancer patients who underwent ^{68}Ga-FAPI PET/MRI after NAC at the University Hospital Münster from May 2020 to May 2021. No exclusion criteria were applied. The baseline scans of 12 of the 13 patients were previously reported (*10*).

Radiochemistry

Application and production of ^{68}Ga-FAPI were performed according to the German Pharmaceuticals Act §13(2b). Precursor was kindly provided under a material transfer agreement by Uwe Haberkorn (Heidelberg, Germany), and radiolabeling was performed as previously described (*10*).

Imaging

Women were injected intravenously with 99 ± 33 MBq (mean ± SD) of ^{68}Ga-FAPI and examined in a hybrid PET/MRI 3-T scanner with a 4-channel dedicated PET/MRI breast coil (mMR; Siemens Healthineers). Breast list-mode PET (25 min) with the patient prone was started an average of 35 min after injection (range, 23–70 min), combined with a standard breast MRI protocol consisting of the following sequences: transversal T2-weighted turbo spin-echo spectral attenuated inversion recovery, diffusion-weighted imaging, T1-weighted fast low-angle shot contrast-enhanced dynamic imaging (gadobutrol, 0.1 mmol/kg of body weight [Gadovist; Bayer]), and contrast-enhanced high-spatial-resolution fat-saturated T1-weighted fast low-angle shot imaging, as described previously (*10*). In 11 of 13 patients, no whole-body scans were performed and lower radiotracer doses corresponding to 1–1.25 MBq/kg of body weight were injected, compared with baseline doses of 156 ± 51 MBq (*10*). An interim analysis had established unbiased assessment of breast PET/MRI at these reduced doses (Supplemental Figs. 1–3; supplemental materials are available at http://jnm.snmjournals.org).

Image Analysis

Prone single-bed-position follow-up breast PET/MR images after NAC were analyzed. Visual categorization of MRI alone and integrated PET/MRI was performed separately by 3 readers for each modality, with masking of the pathology results. The initial clinical report, finalized before pathology was available, was analyzed in consensus by an MRI reader and a PET/MRI reader: 1 board-certified specialist in radiology (7 y experience in breast imaging) and nuclear medicine (7 y of experience in nuclear oncology). In addition, anonymized imaging studies were separately read as MRI alone and integrated PET/MRI by 2 independent readers: 1 senior trainee and 1 board-certified specialist in radiology (1 and >20 y of experience in breast imaging) and nuclear medicine (3 and >15 y of experience in nuclear oncology), respectively. These individuals were previously not involved in reading the cases. The readers were masked to the clinical report of the follow-up PET/MRI and all data collected afterward but had access to previous examinations, including baseline prone breast PET/MRI and supine whole-body PET/MRI or PET/CT. The MRI readers did not have access to the PET component of follow-up PET/MR images and were given the reports of previous studies when deemed necessary. Integrated PET/MRI readers evaluated the radiotracer uptake and had additional access to the MR images, including interpretation when relevant for tumor bed delineation.

Measurements were performed with spheric and ellipsoid volumes of interest as described previously (*10*). Tumor-to-background ratios ($TBR_{max/max}$) represent the ratio of the lesion and entire contralateral breast SUV_{max} or a healthy part of the ipsilateral breast when patients had prior contralateral mastectomy. Follow-up PET measurements are the means for all readers. Only the main breast lesion and most suggestive LN were considered for analysis.

Breast lesions and LNs were visually assigned to 1 of 3 categories. For MRI of the breast, the categories were no residual tumor or contrast enhancement greater than the background level (category A), possible residual tumor (i.e., faint contrast enhancement) (category B), and probable (>75%) residual tumor (i.e., mass lesion with contrast enhancement) (category C). For MRI of the axilla, the categories were normal LNs (category A), possible metastasis (discrete change or enhancement) (category B), and probable (>75%) metastasis (category C). For PET/MRI of the breast and axilla, the categories were no focal uptake (category A), possible focal uptake and possible background noise (category B), and certain focal uptake (category C). Majority reads were the most prevalent category, or category B if all categories were synchronously selected.

Histology

Pathologic response and immunostaining were assessed as part of the clinical routine according to common standards on resected breast and axillary tissue as reported previously (*10*). pCR in the breast was defined as absence of invasive cancer. One patient had remnant tumor cells in lymphatic vessels only and was classified as no pCR. FAP immunohistochemistry was conducted as described previously (*10*) and categorized as FAP-negative (category A), mildly positive (category B), or intensely positive (category C).

Statistical Analysis

Statistical analysis was performed using Matlab (version R2020a; MathWorks). Mann–Whitney *U* tests were used to compare tracer uptake metrics and FAP immunoreactivity for women with or without pCR and uptake metrics between baseline and follow-up. A P value of less than 0.05 was considered statistically significant. For the optimal threshold in receiver-operating characteristics (ROCs), the costs for false negatives (FN) and false positives (FP) were weighed as 80% and 20%, respectively. The calculation of sensitivity and specificity considered no pCR as positive. Cited diagnostic performance values were adapted when based on an inverse definition.

RESULTS

Patient Characteristics

We analyzed overall 13 follow-up ^{68}Ga-FAPI PET/MRI scans of the breast after completion of NAC for breast cancer in 13 women (nonexcluded) (mean age, 47 ± 9 y). Twelve women received prior baseline ^{68}Ga-FAPI PET/MRI scans, published previously (*10*). PET/MRI was conducted 12 ± 8 d after completion of NAC. Surgery that established the reference standard was conducted 13 ± 5 d after PET/MRI. Seven of 13 women achieved pCR in the breast, 6 of 10 women with LN metastases at baseline achieved axillary pCR, and 7 of 13 achieved overall pCR. More patient characteristics are available in Table 1.

Breast Assessment

Tracer uptake by primary breast lesions in follow-up was markedly decreased to a mean SUV_{max} of 1.8 (range, 0.9–3.5) from the baseline mean SUV_{max} of 14.2 (range, 8.6–29.9) ($P < 0.001$; mean reduction to 12% [range, 4–22]). Breast background uptake was also decreased to a mean SUV_{max} of 1.3 (range, 0.8–2.7) from the baseline mean SUV_{max} of 2.6 (range, 1.1–6.9) ($P = 0.006$; mean reduction to 62% [range, 24–104]). This resulted in a reduced mean $TBR_{max/max}$ of 1.4 (range, 0.6–3.1), compared with a baseline mean $TBR_{max/max}$ of 7.0 (range, 1.9–16.0) ($P < 0.001$) (Fig. 1; Supplemental Table 1; Supplemental Figs. 4 and 5).

TABLE 1
Patient Characteristics

Patient no.	Age (y)	Type	Grade	Receptor status	Systemic therapy	Interval from last cycle to PET (d)
1	56	Ductal	2	HR+, HER2+	AC T H*	15
2	51	Ductal	2	HR+, HER2+	EC T H	15
3	51	Ductal	1	HR+, HER2+	EC T H	6
4	35	Ductal	3	TNBC	EC T Cb	10
5	46	Ductal	3	HR+, HER2−	EC T	6
6	58	Ductal	3	HR−, HER2+	EC T H	0
7	56	Lobular	2	HR+, HER2+	EC T H	29
8	43	Ductal	2	TNBC	T Cb	15
9	38	Ductal	2	HR−, HER2+	EC T H	1
10	36	Lobular	2	HR+, HER2−	EC T	20
11	59	Ductal	2	HR+, HER2−	EC T	14
12	48	Ductal	3	HR−, HER2+	EC T H	15
13	34	Ductal	2	HR+, HER2-	EC T	8

*Additional investigational drug.
HR = hormone receptor; HER2 = human epidermal growth factor receptor 2; TNBC = triple-negative breast cancer; AC = doxorubicin; T = taxane; H = HER2-antibodies; EC = epirubicin; Cb = carboplatin.

For integrated PET/MRI, the primary breast lesion visual categories were consistent in 9 of 13 women among the 3 readers. The readers' majority visual classification resulted in an FN rate of 0, FP rate of 0, sensitivity of 100%, and specificity of 100%, when only category C (certain focal uptake) was defined as positive. Considering categories B (possible focal uptake) and C as positive resulted in an FN rate of 0, FP rate of 2, sensitivity of 100%, and specificity of 71% (Figs. 1, 2C, and 2D; Table 2). Among readers, the SD was 0.1 for lesion and background SUV_{max} and $TBR_{max/max}$. $TBR_{max/max}$ demonstrated perfect classification of remission status (breast pCR: mean $TBR_{max/max}$, 0.9 [range, 0.6–1.2]; no pCR: mean $TBR_{max/max}$, 2.1 [range, 1.4–3.1] [$P = 0.001$]) (ROC optimal threshold $TBR_{max/max}$, 1.4; sensitivity, 100%; specificity, 100%) (Figs. 1, 2A, and 2D). In contrast, SUV_{max} measurements showed relevant overlap between response categories (pCR: mean SUV_{max}, 1.1 [range, 0.9–1.8]; no pCR: mean SUV_{max}, 2.5 [range, 1.3–3.5] [$P = 0.002$]) (ROC optimal threshold SUV_{max}, 1.3; sensitivity, 100%; specificity, 86%) (Figs. 2B and 2D). The relative SUV_{max} reduction from baseline was significantly different, but with a high overlap between response groups in 12 eligible women (pCR: mean reduction to 10% [range, 4%–20%]; no pCR: mean reduction to 16% [range, 10%–22%] [$P = 0.03$]). Baseline SUV_{max} was not significantly different ($P = 0.20$).

In patient 5, the primary breast lesion was not evaluable on MRI because of a marker clip susceptibility artifact. MRI-alone breast lesion categories were consistent in 6 of 12 evaluable women among readers. Majority categorization for MRI resulted

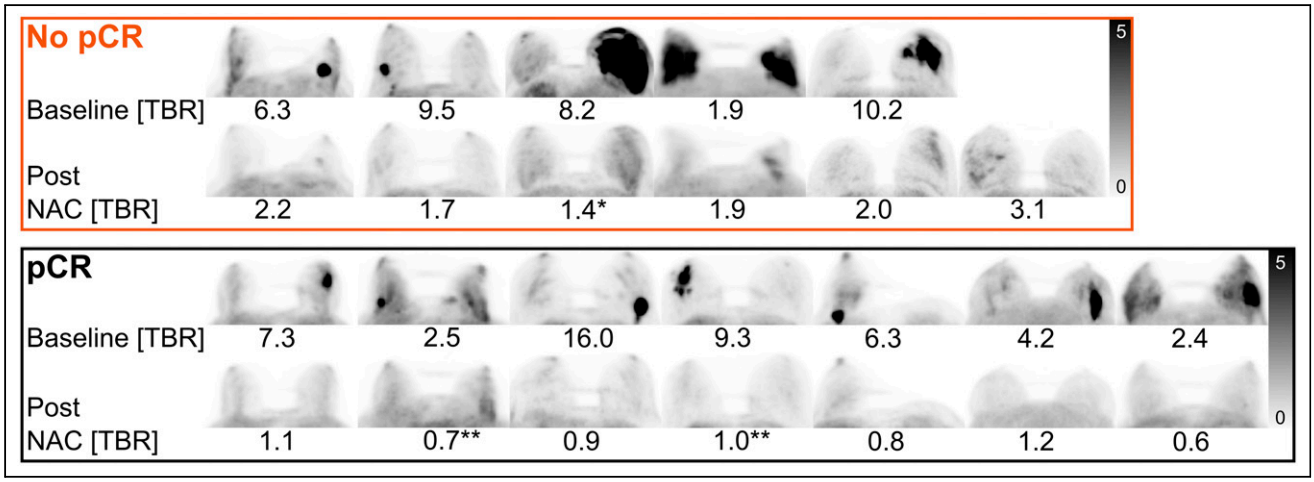

FIGURE 1. Craniocaudal maximum-intensity projections of whole-breast ^{68}Ga-FAPI before and after NAC of patients not achieving or achieving pCR in breast. Patients with no pCR are, from left to right, patients 2, 3, 4, 10, 11, and 13. Patients with pCR are, from left to right, patients 1, 5, 6, 7, 8, 9, and 12. Baseline and post-NAC $TBR_{max/max}$ is given for each patient. All images are tuned to an SUV range of 0–5 (Supplemental Figs. 4 and 5). *No pCR with remnant tumor cells only in lymphatic vessels. **pCR with residual carcinoma in situ.

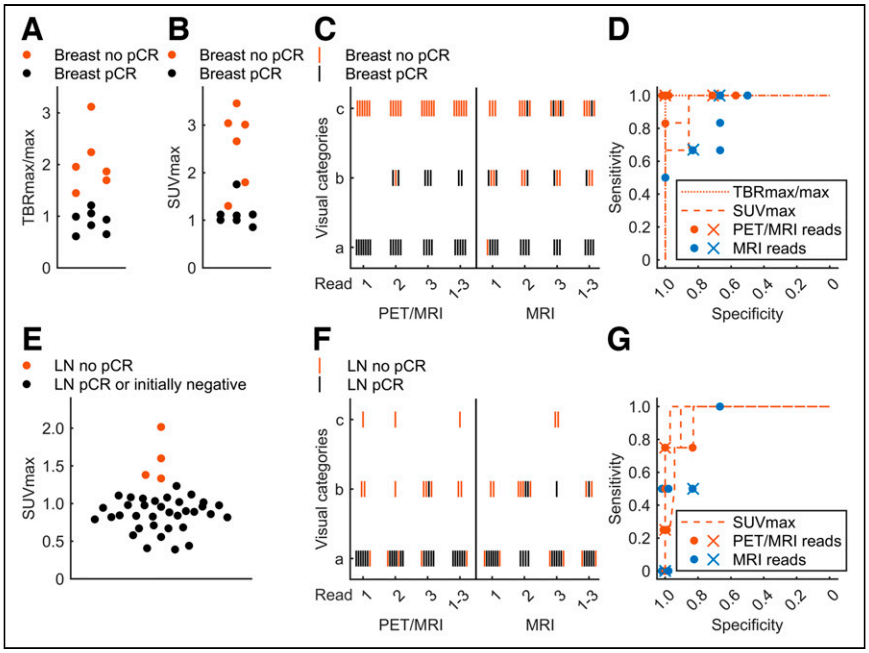

FIGURE 2. (A) Breast lesion $TBR_{max/max}$ bee swarm plots of no pCR and pCR. (B) Corresponding plots by SUV_{max}. (C) Category for breast lesions for individual and majority PET/MRI and MRI reads. (D) ROC curves by $TBR_{max/max}$ or SUV_{max} corresponding to individual measurements of 3 readers. Sensitivity and specificity for individual (dots) and majority (crosses) reads are plotted for PET/MRI and MRI alone either considering categories B and C positive or considering only category C positive. Overlying dots were slightly shifted to allow visualization. (E) Axillary node SUV_{max} for axillary level 1 LNs. (F) Visual assessment category for LNs. (G) ROC curves for LNs with additionally plotted results from individual and majority reads.

in an FN rate of 2, FP rate of 1, sensitivity of 67%, and specificity of 83% when only category C (probable tumor) was defined as positive. Considering categories B (possible tumor) and C as positive led to an FN rate of 0, FP rate of 2, sensitivity of 100%, and specificity of 67% (Figs. 2C and 2D). Figure 3 shows 2 examples of superior visualization of remnant breast cancer by the ^{68}Ga-FAPI PET component compared with MRI alone and of crucial guidance of the MRI component toward correct integrated PET/MRI assessment, respectively.

In 13 patients with available immunohistochemistry, FAP staining categories were associated with remission status (breast pCR: category A [FAP negative], 1/7; category B [mildly positive], 6/7; category C [intensely positive], 0/7) (no pCR: category A, 0/6; category B, 2/6; category C, 4/6) ($P = 0.033$) (Figs. 4A and 4B).

Axillary Assessment

Uptake by LN metastases was reduced after NAC to a mean SUV_{max} of 1.2, (range, 0.8–2.0), compared with a baseline mean SUV_{max} of 10.0 (range, 3.4–18.7) ($P < 0.001$; reduction to 14% [range, 5–40]) (Supplemental Table 2).

TABLE 2
Visual Assessment Categories A–C for Individual Readers

	Breast			LN		
		Follow-up category			Follow-up category	
Patient no.	Response	PET/MRI	MRI	Response	PET/MRI	MRI
1	pCR	**AAA**	**AAA**	pCR	**AAA**	**AAA**
2	No pCR	**CCC**	**CCC**	pCR	**AA**B	A**BB**
3	No pCR	**C**B**C**	B**CC**	NA	NA	NA
4	No pCR*	**CCC**	**BBB**	No pCR	**B**A**B**	**BB**C
5	pCR†	**AAA**	NA‡	pCR	**AAA**	**AAA**
6	pCR	A**BB**	**B**AC	pCR	**AAA**	**AAA**
7	pCR†	**AA**B	**AAA**	pCR	**AAA**	**AAA**
8	pCR	A**BB**	B**CC**	NA	NA	NA
9	pCR	**AAA**	**AA**B	pCR	**AAA**	**AB**A
10	No pCR	**CCC**	**CC**B	No pCR	**AAA**	**AB**A
11	No pCR	**CCC**	A**BB**	No pCR	**BBB**	**BB**C
12	pCR	**AAA**	**AB**A	NA	NA	NA
13	No pCR	**CCC**	**CCC**	No pCR	**CC**B	**AB**A

*No pCR, with remnant tumor cells only in lymphatic vessels.
†pCR, with residual carcinoma in situ.
‡Clip artifact prevented breast assessment.
NA = not applicable.
Majority assessment is highlighted in bold.

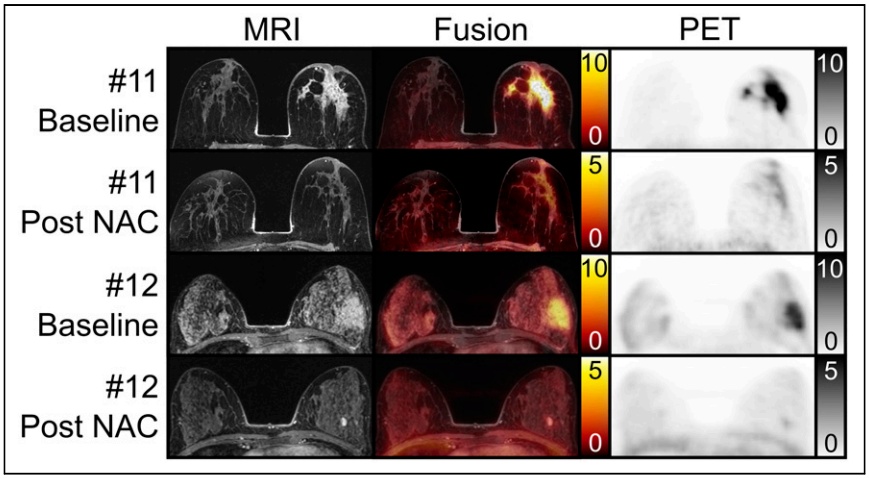

FIGURE 3. Examples of breast lesion patients with prone transverse contrast-enhanced fat-saturated T1-weighted MRI scan, fusion image, and ^{68}Ga-FAPI PET scan at baseline and at follow-up after NAC. In patient 11, follow-up showed extensive remnant ^{68}Ga-FAPI uptake ($TBR_{max/max}$, 2.0) in breast, whereas MRI was negative or slightly positive in circumscribed area near nipple, depending on reader. Pathology revealed remnant 10-cm invasive cancer matching PET assessment. In patient 12, follow-up showed focal mild ^{68}Ga-FAPI and intense MRI contrast enhancement adjacent to tumor bed. MRI characteristics established fibroadenoma, allowing classification of tumor bed as negative on MRI and PET/MRI, later confirmed by pathology.

In integrated PET/MRI, visual assessment of LNs was consistent among readers in 7 of 10 women. Majority classification resulted in an FN rate of 3, FP rate of 0, sensitivity of 25%, and specificity of 100% when only category C was defined as positive. Considering categories B and C as positive resulted in an FN rate of 1, FP of 0, sensitivity of 75%, and specificity of 100% (Figs. 2F and 2G). Among readers, the SD of SUV_{max} measurements of the most intense ipsilateral node was 0.2. Despite imperfect visual assessment, all readers' mean SUV_{max} measurements of LNs could perfectly classify pCR and no pCR in the group of 10 affected women (LN pCR: mean SUV_{max}, 0.9 [range, 0.8–1.1]; no pCR: mean SUV_{max}, 1.6 [range, 1.3–2.0] [$P = 0.001$]) (ROC optimal threshold SUV_{max}, 1.3; sensitivity, 100%; specificity, 100%). Adding up to 29 contralateral and ipsilateral initially nonmetastatic LNs to pCR LNs still resulted in perfect SUV_{max}-based classification (pCR and nonmetastatic LNs: mean SUV_{max}, 0.9 [range, 0.4–1.2]; ROC optimal threshold: SUV_{max}, 1.3; sensitivity, 100%; specificity, 100%) (Fig. 2E). However, when analyzing readers' individual measurements, classification was imperfect (ranges of 3 readers: ROC optimal threshold SUV_{max}, 1.1–1.5; sensitivity, 75%–100%; specificity, 90%–97%) (Fig. 2G). The relative SUV_{max} reduction from baseline was significantly different between response groups in 9 eligible women (pCR: mean reduction to 9% [range, 5%–13%]; no pCR: mean reduction to 23% [range, 14%–40%]; $P = 0.02$). Baseline SUV_{max} was not significantly different ($P = 0.38$).

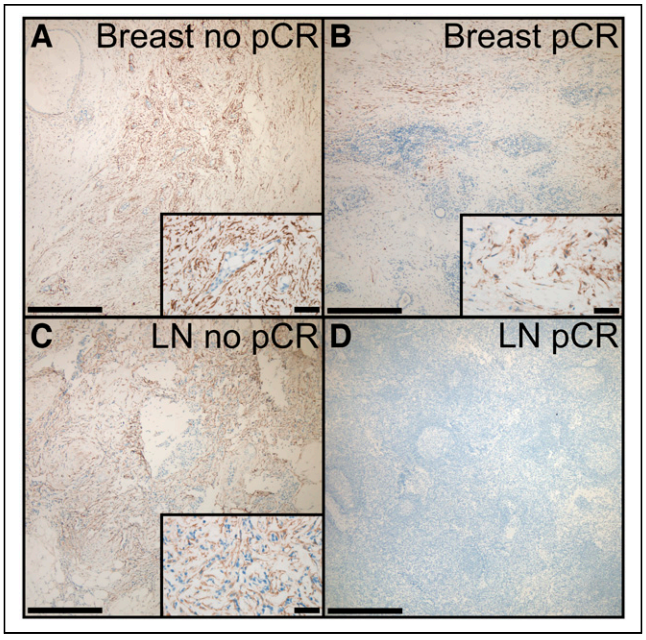

FIGURE 4. Example immunostainings of FAP in breast and LN tissue. (A) Breast no pCR classified as intensely positive (category C), showing clustering of FAP-positive fibroblasts, with area and amount exceeding small areas of remnant cancer cells. (B) Breast pCR with regressive changes and scattered FAP-positive fibroblasts (category B). (C) LN no pCR with remnant cancer cells and intermingled FAP-positive fibroblasts (category C). (D) LN pCR with absence of FAP immunoreactivity (category A). Bars indicate 500 μm for ×4 magnification and 50 μm for ×40 magnification in insets.

MRI-alone readers were consistent in 4 of 10 women. Majority MRI categorization resulted in an FN of 4, FP of 0, sensitivity of 0%, and specificity of 100% when only category C was defined as positive. Considering categories B and C as positive resulted in an FN of 2, FP of 1, sensitivity of 50%, and specificity of 83% (Figs. 2F and 2G). Figure 5 gives 2 examples of better visualization of LN metastases by the MRI and ^{68}Ga-FAPI PET components.

In 8 patients with available immunohistochemistry, LN FAP staining categories were associated with remission status (LN pCR: category A, 4/4; category B, 0/4; category C, 0/4) (no pCR: category A, 0/4; category B, 2/4; category C, 2/4) ($P = 0.029$) (Figs. 4C and 4D).

Combined Assessment

For combined assessment of axillary and breast response status, majority classification resulted in an FN of 0, FP of 0, sensitivity of 100%, and specificity of 100% for PET/MRI and an FN of 2, FP of 1, sensitivity of 67%, and specificity of 86% for MRI alone when only category C was defined as positive. Considering categories B and C as positive resulted in an FN of 0, FP of 2, sensitivity of 100%, and specificity of 71% for both PET/MRI and MRI alone.

DISCUSSION

Currently, no imaging test can identify breast cancer patients with pCR after NAC with sufficient accuracy to allow for deescalation of therapy by abbreviating chemotherapy or even omitting surgery.

In this study, we were the first—to our knowledge—to analyze the diagnostic performance of ^{68}Ga-FAPI PET/MRI in assessing response to NAC in breast cancer. Combined and breast pathologic response could be correctly classified in all 13 patients based on ^{68}Ga-FAPI uptake on PET/MRI, whereas MRI alone assigned at least 2 patients falsely. PET/MRI could also classify LN status

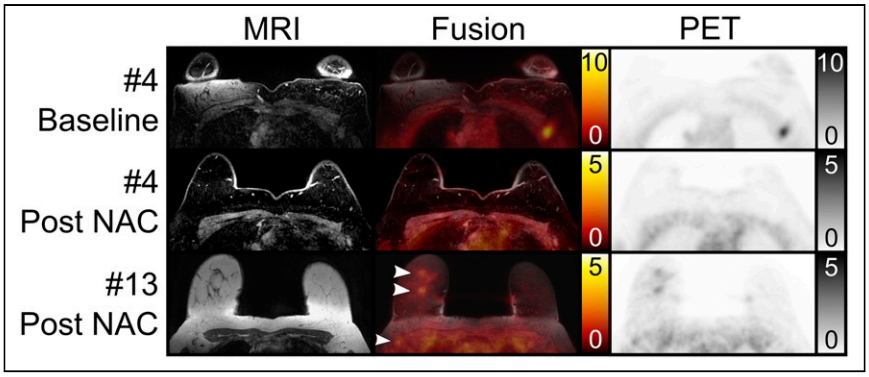

FIGURE 5. Examples of LN metastasis patients with prone transverse contrast-enhanced fat-saturated T1-weighted MRI scan (top and middle MRI rows), native T1-weighted MRI scan (bottom MRI row), fusion image, and ^{68}Ga-FAPI PET scan at baseline and at follow-up after NAC. In patient 4, follow-up showed that nodal remnant tracer uptake was not readily distinguishable from adjacent muscle. This was found to be remnant LN metastasis at pathology, classified as possible focal uptake on PET/MRI and as probable remnant metastasis on MRI. In patient 13, follow-up showed clear breast remnants on PET/MRI and MRI (top 2 arrowheads). PET/MRI, but not MRI, demonstrated clear abnormalities in right axillary nodes (bottom arrowhead), which were found to be remnant metastases at pathology.

correctly in at least 2 more patients than MRI alone. Metaanalyses showed that in the detection of breast cancer remnants after NAC, MRI had a sensitivity of 88%–92% and a specificity at 60%–69% (*13–16*). This makes MRI the most sensitive widely clinically available noninvasive imaging modality. ^{18}F-FDG/PET complements breast MRI not in terms of sensitivity (66%–77%) but in terms of specificity (78%–86%) (*15–17*). In the context of deescalation, FNs are far more important than FPs. The observed trend of FAPI-based assessment to improve sensitivity and specificity is thus particularly remarkable. This trend from our small study sample is substantiated by the observed higher interobserver agreement and correlation with semiquantitative measures of FAP uptake and immunohistochemistry. Furthermore, the observation of a higher number and area of FAP-positive fibroblasts than of vital remnant cancer cells in some specimens provides a strong rationale for our chosen molecular target. In comparison to the breast, for the LNs the conclusions on assessment of remission status are not as clear, considering the nonideal prone breast MRI protocol for axillary nodes with variable image quality and overall less intriguing diagnostic PET/MRI performance. However, it is important to consider that the combination of breast pCR without axillary pCR is rare and appeared in only 3.3% of initially node-positive patients in a review of approximately 20,000 U.S. patients (*18*).

In accordance with the most recent American Society of Clinical Oncology guidelines (*1*), we adopted a pCR definition of absence of invasive cancer, thus allowing remnant in situ cancer in pCR. This owes to the fact that the response rate of, for example, ductal carcinoma in situ (DCIS) (*19,20*) is much lower and that the predictiveness of survival of residual DCIS is not given (*21*) after NAC in contrast to residual invasive cancer. Therefore, in situ cancer can be considered a confounder in NAC and associated deescalation concepts. Although our definition of pCR is probably most appropriate for chemotherapy deescalation, residual DCIS should not be missed in surgical deescalation. It is important to know that an immunohistochemistry study did not find FAP expression in DCIS, in contrast to invasive cancer (*22*). Consistently in our cohort, 2 PET- and MRI-negative women with known carcinoma in situ at baseline had noninvasive remnants despite pCR. Even patients with no DCIS at baseline can have isolated remnant DCIS after NAC, as was found, for example, in approximately 12% of patients (*19,20*) in 2 studies. Thus, when considering FAPI PET/MRI for surgical deescalation in future trials, reliable exclusion of DCIS by breast imaging modalities, such as mammography, would probably be required.

Our study had limitations, the most important one being the low number of patients and its retrospective nature. The obtained diagnostic performance values thus must be considered as trends rather than a true approximation of diagnostic performance. Considering the overlap with our previous publication, our study features the same potential selection bias as discussed previously (*10*). We used ^{68}Ga-FAPI scanning only before and after completion of NAC, whereas the best accuracies in, for example, ^{18}F-FDG PET are achieved in interim response assessments during chemotherapy (*17*). Thus, more appropriate imaging time points may exist for ^{68}Ga-FAPI scanning, particularly if considering its use for chemotherapy deescalation.

CONCLUSION

Integrated ^{68}Ga-FAPI PET/MRI shows highly promising trends toward gains in diagnostic performance over MRI alone to correctly classify response status in the breast and axilla in a small study sample. Future larger prospective studies are warranted to more closely approximate the true diagnostic performance and evaluate whether ^{68}Ga-FAPI PET/MRI ultimately possesses the potential to guide deescalation of chemotherapy or even surgery.

DISCLOSURE

This study was partly funded by the ninth Deutsche Forschungsgemeinschaft (DFG) NAMT, DFG–CRC1450-431460824, Münster, Germany (project B06), and a rotational clinician scientist position of the DFG–CRC1009, Münster, Germany, to Philipp Backhaus. No other potential conflict of interest relevant to this article was reported.

KEY POINTS

QUESTION: Can ^{68}Ga-FAPI PET/MRI classify response status after NAC in breast cancer?

PERTINENT FINDINGS: In a retrospective study of 13 women who completed NAC for breast cancer, follow-up ^{68}Ga-FAPI PET/MRI perfectly assessed the pathologic response status of the breast. MRI alone classified at least 2 women falsely.

IMPLICATIONS FOR PATIENT CARE: The diagnostic performance of ^{68}Ga-FAPI PET/MRI trended toward a gain over MRI alone, clearly supporting future prospective studies.

REFERENCES

1. Korde LA, Somerfield MR, Carey LA, et al. Neoadjuvant chemotherapy, endocrine therapy, and targeted therapy for breast cancer: ASCO guideline. *J Clin Oncol.* 2021;39:1485–1505.

2. Riedel F, Hoffmann AS, Moderow M, et al. Time trends of neoadjuvant chemotherapy for early breast cancer. *Int J Cancer.* 2020;147:3049–3058.
3. Sacchini V, Norton L. Escalating de-escalation in breast cancer treatment. *Breast Cancer Res Treat.* 2022;195:85–90.
4. Heil J, Kuerer HM, Pfob A, et al. Eliminating the breast cancer surgery paradigm after neoadjuvant systemic therapy: current evidence and future challenges. *Ann Oncol.* 2020;31:61–71.
5. Slanetz PJ, Moy L, Baron P, et al. ACR Appropriateness Criteria® monitoring response to neoadjuvant systemic therapy for breast cancer. *J Am Coll Radiol.* 2017;14:S462–S475.
6. Nakashima K, Uematsu T, Harada TL, et al. Can breast MRI and adjunctive Doppler ultrasound improve the accuracy of predicting pathological complete response after neoadjuvant chemotherapy? *Breast Cancer.* 2021;28:1120–1130.
7. Sutton EJ, Braunstein LZ, El-Tamer MB, et al. Accuracy of magnetic resonance imaging–guided biopsy to verify breast cancer pathologic complete response after neoadjuvant chemotherapy. *JAMA Netw Open.* 2021;4:e2034045.
8. Choi JH, Kim H-A, Kim W, et al. Early prediction of neoadjuvant chemotherapy response for advanced breast cancer using PET/MRI image deep learning. *Sci Rep.* 2020;10:21149.
9. Cho N, Im S-A, Cheon GJ, et al. Integrated ^{18}F-FDG PET/MRI in breast cancer: early prediction of response to neoadjuvant chemotherapy. *Eur J Nucl Med Mol Imaging.* 2018;45:328–339.
10. Backhaus P, Burg MC, Roll W, et al. Simultaneous FAPI PET/MRI targeting the fibroblast-activation protein for breast cancer. *Radiology.* 2022;302:39–47.
11. Elboga U, Sahin E, Kus T, et al. Superiority of ^{68}Ga-FAPI PET/CT scan in detecting additional lesions compared to ^{18}FDG PET/CT scan in breast cancer. *Ann Nucl Med.* 2021;35:1321–1331.
12. Kömek H, Can C, Güzel Y, et al. ^{68}Ga-FAPI-04 PET/CT, a new step in breast cancer imaging: a comparative pilot study with the ^{18}F-FDG PET/CT. *Ann Nucl Med.* 2021;35:744–752.
13. Marinovich ML, Houssami N, Macaskill P, et al. Meta-analysis of magnetic resonance imaging in detecting residual breast cancer after neoadjuvant therapy. *J Natl Cancer Inst.* 2013;105:321–333.
14. Yuan Y, Chen X-S, Liu S-Y, Shen K-W. Accuracy of MRI in prediction of pathologic complete remission in breast cancer after preoperative therapy: a meta-analysis. *AJR.* 2010;195:260–268.
15. Liu Q, Wang C, Li P, Liu J, Huang G, Song S. The role of ^{18}F-FDG PET/CT and MRI in assessing pathological complete response to neoadjuvant chemotherapy in patients with breast cancer: a systematic review and meta-analysis. *BioMed Res Int.* 2016;2016:1–10.
16. Li H, Yao L, Jin P, et al. MRI and PET/CT for evaluation of the pathological response to neoadjuvant chemotherapy in breast cancer: a systematic review and meta-analysis. *Breast.* 2018;40:106–115.
17. Wang Y, Zhang C, Liu J, Huang G. Is ^{18}F-FDG PET accurate to predict neoadjuvant therapy response in breast cancer? A meta-analysis. *Breast Cancer Res Treat.* 2012;131:357–369.
18. Fayanju OM, Ren Y, Thomas SM, et al. The clinical significance of breast-only and node-only pathologic complete response (pCR) after neoadjuvant chemotherapy (NACT). *Ann Surg.* 2018;268:591–601.
19. Groen EJ, van der Noordaa MEM, Schaapveld M, et al. Pathologic response of ductal carcinoma in situ to neoadjuvant systemic treatment in HER2-positive breast cancer. *Breast Cancer Res Treat.* 2021;189:213–224.
20. von Minckwitz G, Darb-Esfahani S, Loibl S, et al. Responsiveness of adjacent ductal carcinoma in situ and changes in HER2 status after neoadjuvant chemotherapy/trastuzumab treatment in early breast cancer: results from the GeparQuattro study (GBG 40). *Breast Cancer Res Treat.* 2012;132:863–870.
21. Mazouni C, Peintinger F, Wan-Kau S, et al. Residual ductal carcinoma in situ in patients with complete eradication of invasive breast cancer after neoadjuvant chemotherapy does not adversely affect patient outcome. *J Clin Oncol.* 2007;25:2650–2655.
22. Hua X, Yu L, Huang X, Liao Z, Xian Q. Expression and role of fibroblast activation protein-alpha in microinvasive breast carcinoma. *Diagn Pathol.* 2011;6:111.